Single Disulfide and Linear Analogues Corresponding to the Carboxy-Terminal Segment of Bovine β-Defensin-2: Effects of Introducing the β-Hairpin Nucleating Sequence D-Pro-Gly on Antibacterial Activity and Biophysical Properties†

Viswanatha Krishnakumari, Ambure Sharadadevi, Shashi Singh, and Ramakrishnan Nagaraj*

Centre for Cellular and Molecular Biology, Uppal Road, Hyderabad 500 007, India

Received March 12, 2003; Revised Manuscript Received June 17, 2003

ABSTRACT: Mammalian defensins (α as well as β forms) have a β-hairpin structural motif spanning approximately 20 residues at the carboxy-terminal end. We have investigated the antibacterial activity and biophysical properties of synthetic peptides corresponding to the carboxy-terminal segment of bovine β-defensin-2 (BNBD-2): VRNHVTC$_1$RINRGFC$_2$VPIRC$_3$PGRTRQIGTC$_4$FGPRIKC$_5$C$_6$RSW (positions of disulfide bonds are C$_1$−C$_5$, C$_2$−C$_4$, and C$_3$−C$_6$). The parent sequence chosen was RCPGRTRQIGTIF-GPRIKCRSW (P1), which spans the carboxy-terminal region of BNBD-2. Since the dipeptide sequence D-Pro-Gly favors nucleation of β-hairpin structures even in acyclic peptides, analogues of P1 with one D-Pro-Gly at the central portion and two D-Pro-Gly segments near the N- and C-terminal ends were generated. An analogue in which GP (residues 14 and 15) in P1 was switched to PG was also synthesized. It was observed that the cyclic form as well as their linear forms exhibited antibacterial activity. Circular dichroism and theoretical studies indicated that while the β-hairpin conformation is populated, there is conformational plasticity in the cyclic and linear peptides. The mode of bacterial killing was by membrane permeabilization. The entire mammalian defensin sequence does not appear to be essential for manifestation of antibacterial activity. Hence, short peptides corresponding to the C-terminal segments of mammalian defensins could have potential as therapeutic agents.

Mammalian defensins are key players in host defense against microbial infections (*1*−*7*). These peptides have three disulfide bridges, and depending on the cysteine connectivities (*5*, *6*), they have been classified as α- or β-defensins. New variants called θ-defensins have also been identified (*8*−*10*). These variants, in addition to the three disulfide bridges, also have a cyclic peptide backbone. The structures of several defensins have been determined in solution by nuclear magnetic resonance (NMR) spectroscopy (*11*−*15*) and in the solid state by X-ray crystallography (*16*−*18*). A common conformational feature that is apparent in all of the structures is a β-hairpin comprised of ∼18−20 amino acids spanning approximately two-thirds of the C-terminal segment. In human neutrophil α-defensin HNP-3, the N-terminal segment participates in a triple-stranded β-sheet (*16*). NMR studies have indicated similar structures for other α-defensins (*11*−*13*) as well as the β-defensin bovine neutrophil defensin BNBD-12 (*14*). In human β-defensins 1 and 2, there is a short segment in helical conformation at the N-terminus (*15*, *17*, *18*). The primary structures of α- and β-defensins from several mammalian species have been determined (*19*−*25*). Apart from the disulfide pattern and certain conserved residues, there are considerable variations in the net positive charge (at neutral pH) and peptide chain length. The antimicrobial spectra and salt sensitivity to antimicrobial activity also vary considerably (*1*, *23*, *26*−*29*). We have shown that all of the three disulfides in the α-defensins NP-2 and HNP-1 (*30*, *31*) and β-defensin BNBD-12 (*32*) are not essential for manifestation of antibacterial activity, as two and single disulfide variants also exhibit activity. Even when all of the three disulfide bridges are present, the arrangement as in the native peptides is not necessary for activity. In several β-defensins (*17*, *23*), there is a proline−glycine (PG) sequence after the third cysteine and glycine−proline (GP) sequence proximal to the fourth cysteine. Detailed analyses of high-resolution protein crystal structures with respect to β-hairpin conformation have revealed that amino acids such as glycine and proline have high propensity to occur in the loop region of β-hairpin structures (*33*−*35*). Recent studies have established that the D-proline−glycine (^{D}PG) sequence promotes β-hairpin formation in peptides (*36*−*41*). Since a β-hairpin conformation is a conserved structural motif in β-defensins (*14*, *15*, *17*, *18*), we have investigated the effects of introducing ^{D}PG in the C-terminal 18−40 segment of BNBD-2 on conformation, antibacterial activitiy, and interaction with model membranes. The sequences of the synthetic peptides are shown in Figure 1.

MATERIALS AND METHODS

Materials. 4-(Hydroxymethyl)phenoxyacetamidomethyl-resin (HMPA) and 9-fluorenylmethoxycarbonyl (F-moc) amino acids were obtained from Applied Biosystems (Foster

† This work was partially supported by a grant from the Department of Biotechnology, India (BT/PRO816/HRD/15/78/97).

* To whom correspondence should be addressed. Tel: +91-40-27192589. Fax: +91-40-27160591/27160311. E-mail: nraj@ccmb.res.in.

10.1021/bi034403y CCC: $25.00
Published on Web 07/16/2003

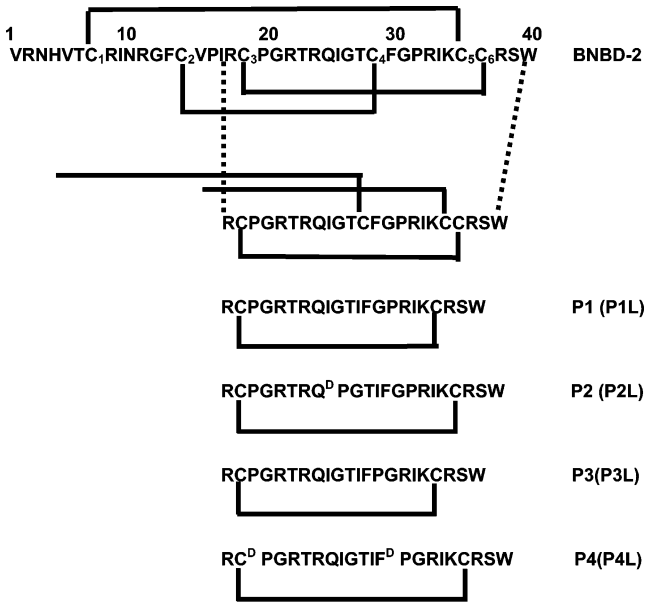

FIGURE 1: Sequences of BNBD-2 and synthetic peptides. Disulfide linkages are shown by solid lines. Peptides P1L−P4L (in parentheses) are linear forms of P1−P4 where the cysteine side chain protecting group acm has been retained.

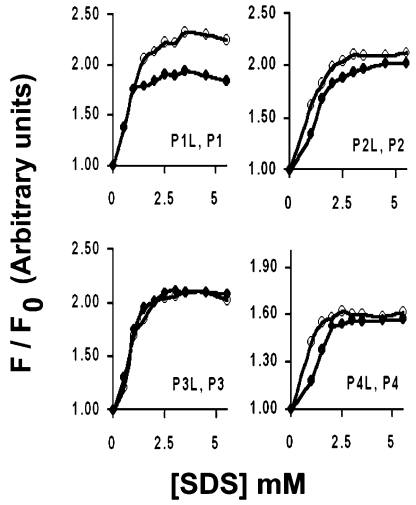

FIGURE 2: Interaction of linear and cyclic peptides with SDS micelles. Different concentrations of SDS were added to a fixed concentration of peptide (4 μM). Trp fluorescence was monitored. F and F_0 correspond to fluorescence intensities at λ_{max} in the presence and absence of SDS. Key: (○) linear peptides; (●) cyclic peptides.

City, CA) and Novabiochem AG (Switzerland), respectively. *N*-Hydroxybenzotriazole hydrate (HOBT) and 2-(1*H*-benzotriazol-1-yl)-1,1,3,3-tetramethyluronium hexafluorophosphate (HBTU) were from Advanced Chemtech (Louisville, KY). Reagents for deprotection of peptides were purchased from Sigma Chemical Co. (St. Louis, MO). 3,3′-Dipropylthiocarbocyanine iodide [diS-C_3-(5)] and dansyl-PE[1] were purchased from Molecular Probes (Eugene, OR). Lipids were purchased from Avanti Polar Lipids (Alabaster, AL).

Peptide Synthesis. Peptides were synthesized by solid-phase methods manually, using HMPA resin employing Fmoc chemistry (*42*). Peptides were cleaved from the resin using trifluoroacetic acid containing thioanisole, *m*-cresol, and ethanedithiol (10:1, 1:0.5 v/v). The acetamidomethyl (acm) group which was used to protect the side chain in cysteines was removed by treatment with mercuric acetate as described (*43*). Formation of disulfide bonds was accomplished by oxidation in 20% aqueous dimethyl sulfoxide (*44*) at a concentration of 0.5 mg/mL for 24 h at room temperature. Peptides were purified by HPLC on a reverse-phase C-18 column using gradients of solvents: (A) 0.1% TFA in H_2O; (B) 0.1% TFA in CH_3CN. Purified peptides were characterized by matrix-assisted laser-desorption ionization time-of-flight mass spectrometry on a Kratos PC-Kompact MALDI 4VI.102 mass spectrometer using recrystallized α-cyano-4-hydroxycinnamic acid as matrix.

Circular Dichroism (*CD*). Spectra were recorded in 5 mM HEPES buffer (pH 7.4), TFE, and SDS micelles on a JASCO J-715 automatic recording spectropolarimeter at 25 °C using a quartz cell of 1 mm path length. Data are represented as mean residue ellipticities. Peptide concentrations were 100 μM in buffer and SDS micelles and 50 μM in TFE.

Theoretical Methods. Homology modeling, energy minimization, and molecular dynamics studies were carried out on Silicon Graphics Octane workstation using the DISCOVER module of Insight II from Molecular Simulation Inc. (MSI) with CVFF force fields. The sequence of peptide P1 was aligned with the C-terminal portion of human β-defensin-2 (hBD-2), whose structure has been determined in the solid state by X-ray crystallography (*17*). The structure was refined using the REFINE module of HOMOLOGY. The structure was optimized for 50 iterations using a steepest descent minimizer to obtain a maximum derivative of 5 kcal/Å (excluding cross or morse terms) followed by 100 iterations of conjugate gradient minimizer to obtain 1 kcal/Å convergence. The structure was then relaxed for 500 iterations (including cross and morse terms) to achieve a convergence of 0.1 kcal/ Å. The linear structures were obtained by excluding the disulfide bridge. The analogues P2−P4 were constructed using the BIOPOLYMER module of Insight II. Molecular dynamics simulations (MDS) were carried out as follows: The initial structures of peptides P1−P4 and their linear forms were subjected to optimization of 3000 iterations using a combination protocol of minimizers, namely, steepest descent, conjugate gradient, and Newton−Raphson algorithms, until a final convergence of 0.001 kcal/Å was achieved. This was followed by a short equilibration dynamics run of 5 ps at 298 K. The structures were then subjected to a 1 ns dynamics run at this temperature. Structures were stored every 200 fs.

Antibacterial Activity. Bacterial strains used were *Escherichia coli* W 160.37, *Staphylococcus aureus* (ATCC 8530), and *Pseudomonas aeruginosa* (NCTC 6751). The antibacterial activity of the peptides was examined in sterile 96-well plates in a final volume of 100 μL as follows: Bacteria were grown in nutrient broth (Bacto Difco nutrient broth) to mid-log phase and diluted to 10^6 colony-forming units (cfu)/mL in 10 mM sodium phosphate buffer (pH 7.4). Bacteria were incubated with different concentrations of peptides (0.5−20

[1] Abbreviations: CD, circular dichroism; dansyl-PE, egg yolk *N*-{5-[(dimethylamino)naphthyl]-1-sulfonyl}-L-α-phosphatidylethanolamine; HEPES, *N*-(2-hydroxyethyl)piperazine-*N*′-2-ethanesulfonic acid; HPLC, high-performance liquid chromatography; LUV, large unilamellar vesicles; POPC, 1-palmitoyl-2-oleoyl-*sn*-glycerophosphocholine; POPE, 1-palmitoyl-2-oleoyl-*sn*-glycerophosphoethanolamine; POPG, 1-palmitoyl-2-oleoyl-*sn*-glycerophosphoglycerol; SDS, sodium dodecyl sulfate; TFE, trifluoroethanol.

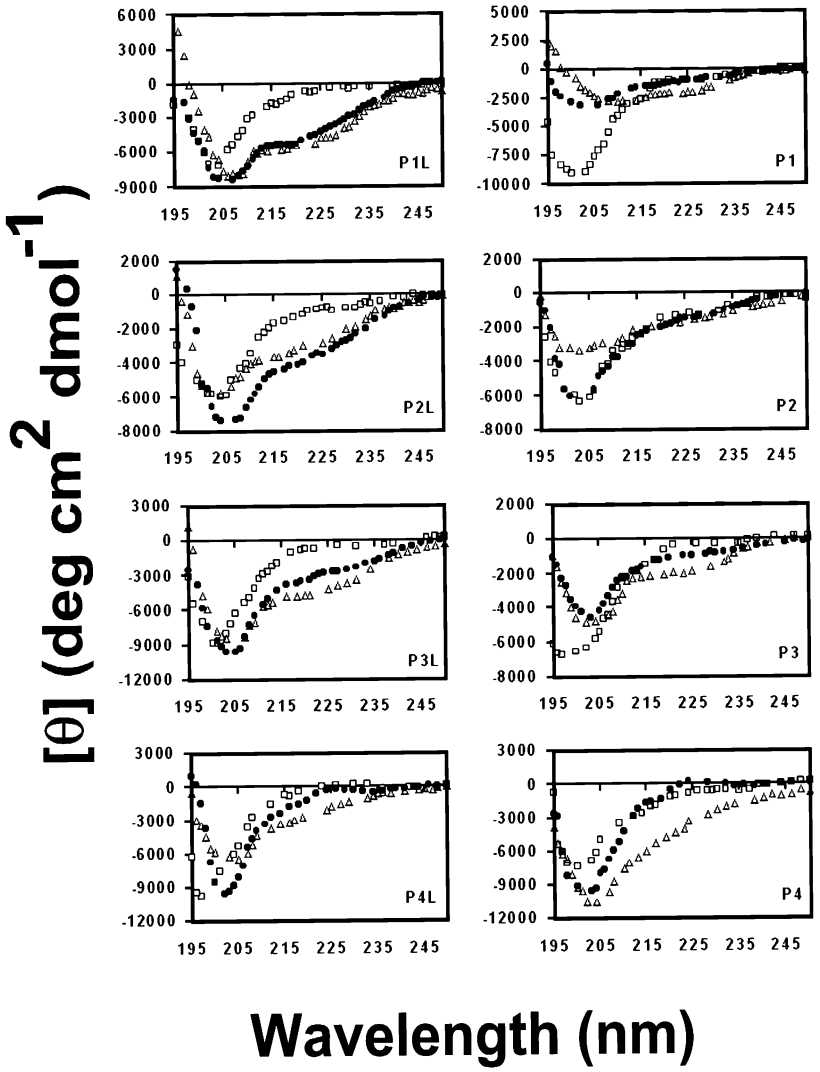

FIGURE 3: Circular dichroism spectra of linear and cyclic peptides. Spectra were recorded in 5 mM HEPES buffer, pH 7.4, and in 10 mM SDS micelles. Key: (□) buffer; (●) SDS micelles; (△) TFE. Concentrations of peptides in buffer and SDS micelles were 100 μM and 50 μM in TFE.

μM) for 2 h at 37 °C, and suitably diluted aliquots were plated on nutrient agar plates. After the plates were incubated at 37 °C for 18 h, colonies formed were counted. The concentration of the peptides at which no viable colonies were formed was taken as lethal concentration (LC). The average of two independent experiments done in duplicate was determined for LC. To determine the effect of salt on antibacterial activity, 150 mM NaCl was included in the incubation buffer.

Electron Microscopy. Bacteria were incubated with peptides at 50% LC as described above and centrifuged at 1500*g* for 3 min. The pellet was fixed in 2.5% glutaraldehyde in 0.1 M phosphate buffer for 3 h at 4 °C. After fixation and washing with 0.1 M phosphate buffer, the samples were then postfixed with 1% osmium tetroxide in 0.1 M phosphate buffer for 2 h. Fixed samples were washed thoroughly with phosphate buffer, following which they were dehydrated through a series of acetone gradients. Dehydrated samples were passed through propylene oxide and infiltrated with epoxy resin overnight. Samples were then embedded in pure epoxy resin and cured at 60 °C for 72 h. Sections were obtained using a Reichert Ultracut E Microtome and were stained with 2% uranyl acetate and Reynold's lead citrate. Sections were observed in a JEOL 100 CX electron microscope at 80 kV using a 20 μm aperture. Control samples without peptides were processed in the same manner.

Binding of Peptides to Micelles and Lipid Vesicles. Binding was assessed by monitoring the fluorescence of tryptophan in the presence of SDS micelles and lipid vesicles composed of POPC and POPE:POPG (3:1 molar ratio). The excitation monochromator was set at 280 nm. The slit width was 5 nm. All measurements were carried out on a F 4500 Hitachi fluorescence spectrometer. LUV were prepared by extrusion through polycarbonate filters (100 nm pore filter) in a miniextruder as described by MacDonald et al. (*45*). Resonance energy transfer experiments were carried out with lipid vesicles doped with 5 mol % of dansyl-PE.

Permeabilization of Lipid Vesicles. The ability of peptides to permeabilize model membranes was examined by monitoring the dissipation of diffusion potential set up in lipid vesicles by valinomycin (*46*). Lipid vesicles with entrapped K^+ were diluted into 5 mM HEPES buffer, pH 7.4, followed by addition of cyanine dye, valinomycin, and peptides. The cyanine dye diS-C_3-(5) (*46*) was used in these experiments. The excitation and emission wavelengths were 620 and 670 nm, respectively. The percentage of fluorescence *F* recovery

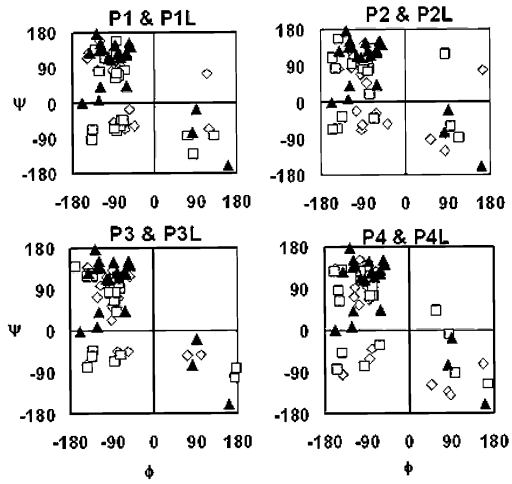

FIGURE 4: Backbone dihedral angles in the structures of P1−P4 and P1L−P4L after Molecular Dynamics Simulations (MDS). Dihedral angles ϕ, ψ of structures after 1 ns MDS are compared along with those of hBD-2 (PDB reference, 1FDA). Key: (◇) peptides with disulfide bridge; (□) linear peptides; (▲) hBD-2, C-terminal segment.

was calculated by using the equation

$$F = [(F_t - F_0)/(F_f - F_0)] \times 100$$

where F_t is the fluorescence observed after addition of peptide at time t, F_0 is the fluorescence after addition of valinomycin, and F_f is the total fluorescence prior to the addition of valinomycin.

RESULTS AND DISCUSSION

Choice of Peptides. The primary structures of the peptides chosen for the study are shown in Figure 1. Peptide P1 corresponds to the sequence C-terminal fragment of BNBD-2 spanning the region linked by a disulfide bridge between cysteines C_3 and C_6. Cysteine C_5 which is connected to C_1 was not included, and C_3 which is connected to C_2 was replaced by isoleucine. This segment also has six of the nine cationic amino acids present in BNBD-2. In P2, this isoleucine was replaced by D-proline with a view to examine the propensity of the peptide to adopt a well-ordered β-hairpin structure, as the ^{D}PG sequence has been demonstrated to induce a well-defined β-hairpin structure in peptides (*36*−*41*). In peptide P3, the GP sequence at positions 14 and 15 was reversed to PG, and the prolines in them were replaced by D-proline in P4. Oxidation of all of the peptides was carried out in 20% aqueous DMSO as described. Oxidation proceeded smoothly in all of the peptides, and under the conditions employed only monomers were obtained. Linear forms P1L−P4L have the acm protecting group.

Conformation of Peptides. The conformations of linear and disulfide-bridged peptides were examined in aqueous environment, TFE, and micelles of SDS, which provides a membrane-like environment and has been used extensively to delineate conformations of peptides in the membrane environment (*47*−*50*). The binding of peptides to SDS micelles was also examined by monitoring tryptophan fluorescence (Figure 2). Considerable increase in F/F_0 as a function of SDS concentration indicates that the peptides bind to SDS micelles.

The CD spectra of linear and disulfide-bridged peptides are shown in Figure 3. In buffer, the linear peptides show spectra characteristic of a large fraction of peptide molecules populating an unordered conformation. In TFE, P1L shows negative minima at ~205 and 225 nm with a crossover at ~200 nm. The spectrum is similar to peptides populating helical and β-hairpin conformation (*51*−*53*) and defensins with three disulfide bridges (*54*−*57*). Introduction of ^{D}PG

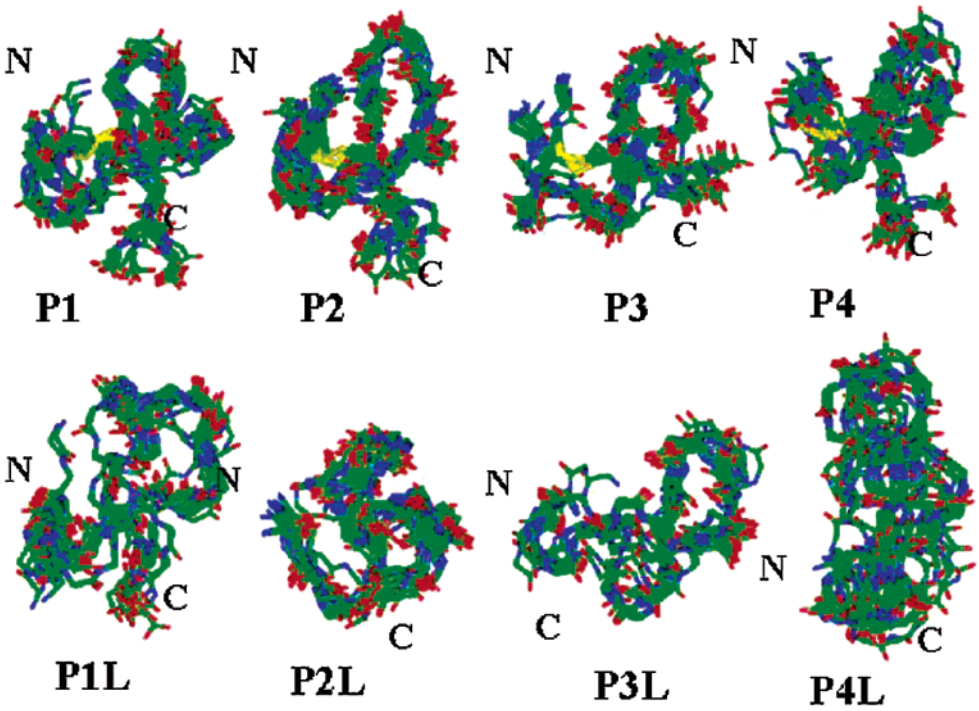

FIGURE 5: Structures of P1−P4 and their linear forms after MDS. Minimum energy structures at intervals of ~500 fs were superimposed. N and C denote amino and carboxy terminus. The carbon, nitrogen, and oxygen atoms are shown in green, blue, and red, respectively. The disulfide bridges are shown in yellow.

Table 1: Antibacterial Activity of Linear and Cyclic Variants of BNBD-2

peptide	lethal concentration (μM)		
	E. coli	*P. aeruginosa*	*S. aureus*
P1L	4	5	5
P1	4	6	4
P2L	4	4	5
P2	4	4	4
P3L	4	5	6
P3	10	7	6
P4L	4	10	6
P4	4	5	6

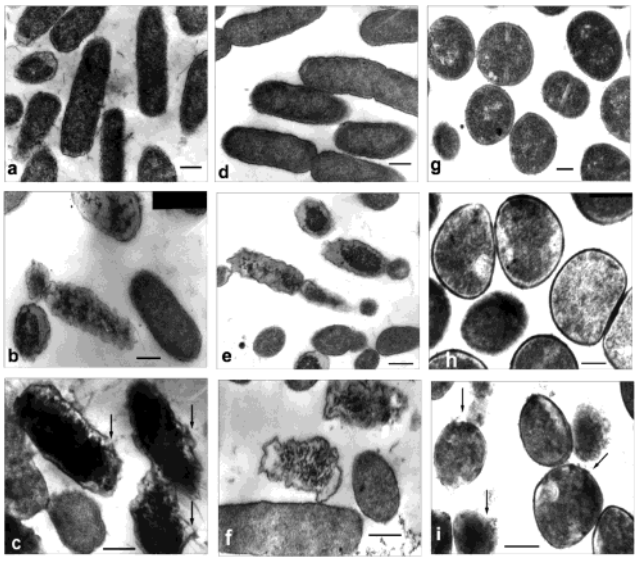

FIGURE 6: Effect of peptides on bacteria visualized by transmission electron microscopy: (a) *E. coli* control; (b, c) after incubation with P1L and P1; (d) *P. aeruginosa* control; (e, f) after incubation with P1L and P1; (g) *S. aureus* control; (h, i), after incubation with P1L and P1. Arrows indicate breaks in the membrane. The bar represents 100 nm. Bacteria were incubated with peptides at 50% lethal concentration as described in Materials and Methods.

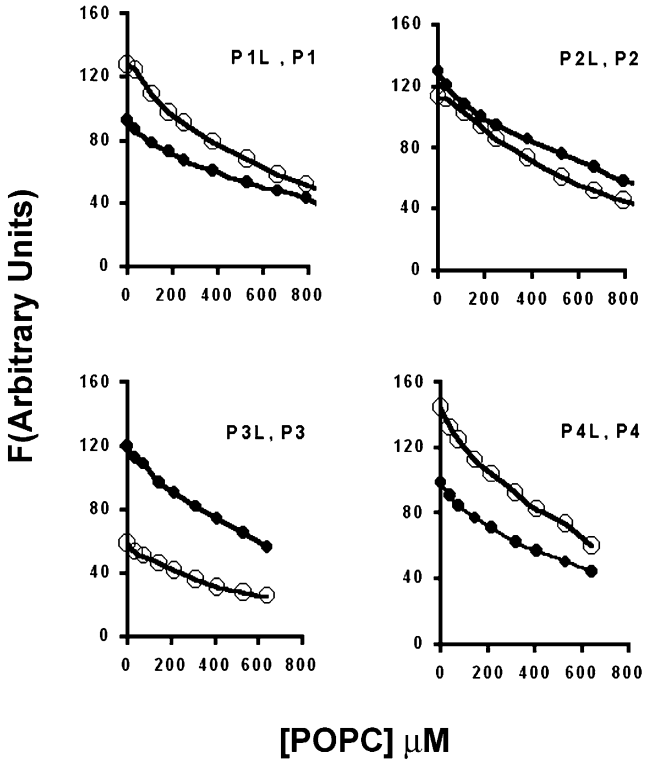

FIGURE 7: Interaction of peptides with POPC LUV. Different concentrations of POPC LUV were added to a fixed concentration of peptide (4 μM). The decrease in fluorescence at λ_{max} is plotted against lipid concentration. Key: (●) cyclic peptides; (○) linear peptides.

and switching of GP to PG appears to favor β-hairpin conformation even in the linear peptides. The spectra of peptides in SDS micelles also suggest β-hairpin conformation.

When the disulfide bridge is formed, spectra of peptides P1, P2, and P4 indicate β-hairpin formation even in aqueous medium. Peptide P3, where GP has been switched to PG is unordered. In TFE and SDS micelles, spectra of P2, P3, and P4 fold into a β-hairpin structure whereas there appears to be a mixed population of helical and β-hairpin structures in the case of P1. CD spectra indicate that introduction of ^{D}PG favors β-hairpin conformation even in aqueous medium. When the GP to PG change is introduced, the β-hairpin structure is observed in TFE and SDS micelles.

The appearance of CD spectra of peptides in the β-hairpin conformation depends on the extent to which the β-hairpin is frayed and, consequently, on the fraction of molecules populating ordered conformation (*53*). Although the CD spectra of P1−P4 and their linear variants suggest preference for the β-hairpin conformation, the wavelength at which crossover occurs and the ellipticity values at the extreme are indicative of structural plasticity as a result of the flexible β-hairpin conformation.

The structure of hBD-2 has been determined in the solid state (*17*). An initial structure for BNBD-2 and analogues was obtained by homology modeling from this structure. This structure was subjected to MDS of 1 ns. A similar strategy was employed to generate the structures for the analogues of BNBD-2. The conformations of the linear peptides were obtained by breaking the disulfide bond, minimizing the energy, and carrying out MDS for 1 ns. The ϕ, ψ angles for a minimum energy structure obtained after 1 ns MDS for the S−S bridged and the linear peptides are shown in Figure 4. The angles for the hBD-2 structure are shown for comparison. It is evident that the angles for some of the residues fall into the "helix" region after MDS in BNBD-2 and analogues. This indicates the tendency for the β-hairpin segment to unfold even though constrained by a disulfide bridge. The superimposed minimum energy structures (backbone atoms) during 1 ns dynamics are shown in Figure 5. It is evident that the disulfide-constrained peptides exhibit conformational plasticity, and introduction of ^{D}P and switching of PG to GP have pronounced effects on peptide conformation. Although the topographies of the linear peptides are different from the disulfide-constrained peptides, chain reversal or a "loose turn" conformation is still evident except in P4L. None of the peptides show NH−CO hydrogen bonds characteristic of the various classified β-hairpin conformations (*33*, *34*). It appears that a single disulfide bridge would not be sufficient to constrain the C-terminal segment of BNBD-2 and possibly even in other β-defensins in a rigid β-hairpin conformation when all of the three disulfide bridges are present. The CD data and theoretical analysis suggest an equilibrium of β-hairpin and unfolded conformation for peptides P1−P4 and their linear forms.

Antibacterial Activity. The relationship between structure and antibacterial activitiy was examined next. The antibacte-

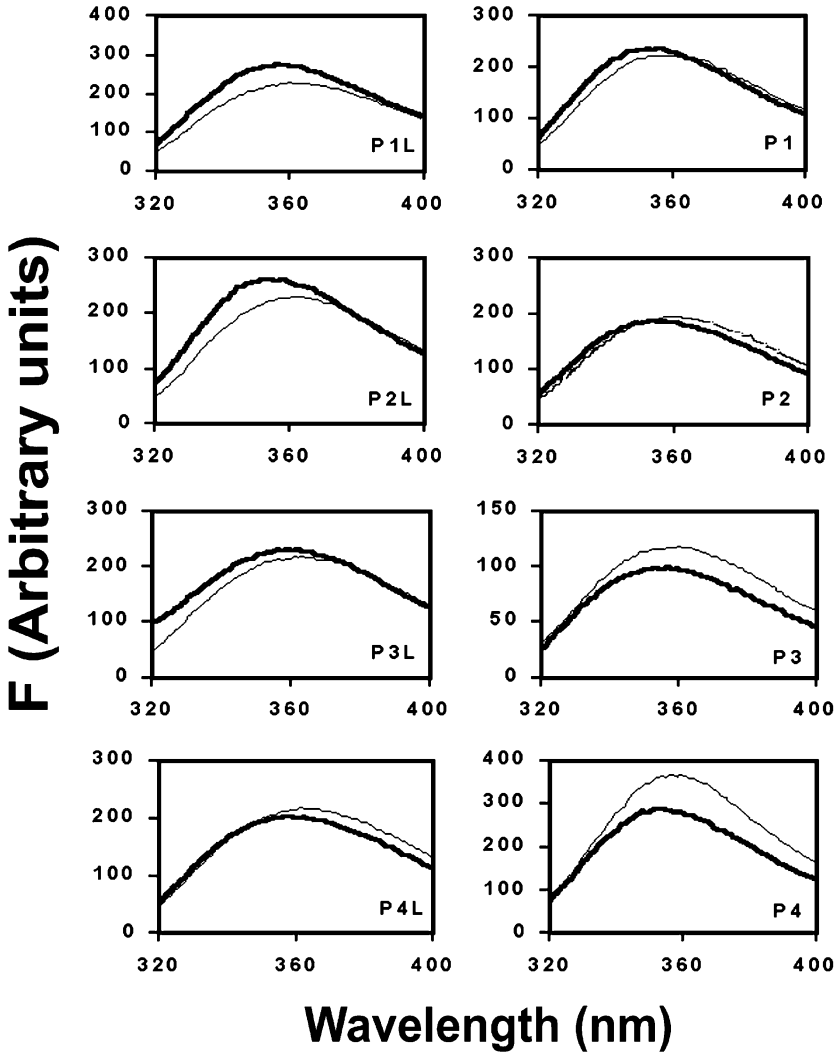

FIGURE 8: Interaction of peptides with PE:PG (3:1) LUV. Fluorescence spectra of peptide in buffer (thin line) and in the presence of PE:PG lipid vesicles (thick line). A fixed concentration of peptide (4 μM) was titrated with increasing concentrations of lipid vesicles. The data presented are maximal changes observed at lipid:peptide ratios of 1:15.

rial activity of the peptides represented as lethal concentrations is summarized in Table 1. All of the linear and cyclic peptides, except P3, exhibited activity at comparable concentrations against *E. coli*. P3 was ~2.5-fold less active. With the exception of P2L, P2, and P3, the peptides exhibited slightly lower activity against *P. aeruginosa* as compared to *E. coli*. The linear and disulfide-bridged peptides were also active against *S. aureus*. At half the lethal concentration, about 60−70% inhibition of growth was observed. All of the peptides did not inhibit the growth of bacteria when 150 mM NaCl was present at the indicated lethal concentrations. About 5−6-fold higher concentration of peptides was necessary to inhibit growth in the presence of salt. However, the peptides were not effective in killing *P. aeuroginosa* in the presence of high salt even at high peptide concentrations. The antibacterial activity of human β-defensins, especially β-defensins-1 and -2, is inhibited at high salt concentrations (*26*−*29*). The salt-sensitive antibacterial activity of peptides corresponding to the C-terminal segment of BNBD-2 suggests that this region could conceivably be an important determinant of antibacterial activity in β-defensins. Peptides corresponding to the C-terminal region of defensins could also be useful in determining the mechanism of salt inactivation of the antibacterial activity of defensins.

The effect of treating *E. coli*, *P. aeruginosa*, and *S. aureus* with P1 and P1L was examined by transmission electron microscopy (Figure 6). At 50% lethal concentration, distinctive changes in morphology are clearly observed. Cytoplasmic contents in the cells tend to cluster. Membrane integrity is compromised as indicated by the arrows. In *S. aureus*, vacuoles in the cytoplasm are discernible along with mesosome-like membranes.

Binding to Model Membranes. Rabbit α-defensin NP-1 has been shown to form voltage-dependent ion-permeable channels in planar lipid bilayers (*58*). Human and rabbit α-defensins bind to negatively charged model membranes in preference to zwitterionic model membranes (*59*−*62*) and cause membrane permeabilization by forming multimeric pores (*59*). Since the BNBD-2 segment and analogues described in Figure 1 have six of the nine cationic amino acids present in the parent peptide, their interactions with model membranes were investigated.

The binding of peptides to lipid vesicles composed of PC and PE:PG (3:1) was examined by monitoring the emission spectra of the tryptophan fluorophore. In buffer, all of the peptides showed a λ_{max} of 355 nm, indicating exposure of the fluorophore to aqueous environment. When the peptides were titrated with increasing concentrations of PC vesicles,

no shift in the position of λ_{max} was observed. There was, however, quenching of fluorescence with increasing lipid concentration (Figure 7). Both the linear and cyclic peptides exhibited similar behavior. The quantum yield in the absence of lipids varies considerably in peptides P3 and P3L. It has been suggested that intermolecular quenching of Trp fluorescence can occur due to quenching by peptide bonds (*63*, *64*). Since the conformation of the peptides varies in aqueous medium, it is likely that this mechanism of quenching may operate in aqueous medium. However, since quenching is observed in all of the peptides in the presence of lipids, other mechanisms may be operative (*65*−*67*). Single phosphate groups from phospholipids have been reported to have the ability to quench fluorescence of tryptophan in peptides (*65*−*67*). In a recent study, the quenching of tryptophan fluorescence in the antibiotic nisin has been attributed to phosphate groups (*67*). It is unlikely that quenching is due to intermolecular interactions as quenching was also observed at high lipid:peptide ratios of 1000:1 (data not shown). We attribute the quenching of Trp fluorescence in all of the peptides as a result of localization of the fluorophore near the phosphate of the headgroup.

The fluorescence spectra of the peptides were examined in the presence of PE:PG (3:1) vesicles (Figure 8). The spectra were recorded at lipid:peptide ratios where maximal changes were observed. The spectra indicate variation in the fluorescence behavior in the peptides. A small blue shift is observed for all of the linear peptides. While in P1L−P3L there is enhancement in intensity, there is a slight quenching in P4L. Peptides P1 and P2 show blue shifts with very little change in intensity whereas P3 and P4 show quenching of fluorescence. The location of Trp in the peptides in PE:PG vesicles appears to be different from PC vesicles. The interaction of P1 and P1L with PE:PG vesicles was further examined by monitoring energy transfer between tryptophan and dansyl fluorophore in lipid vesicles doped with dansyl-PE (Figure 9). Significant energy transfer was observed, indicating that the linear and disulfide-constrained peptides bind to PE:PG vesicles. Since the antibacterial activity of all of the peptides is compromised by high salt, energy transfer in the presence of salt was examined. Considerable reduction in energy transfer was observed (data not shown), suggesting that the peptides do not bind to lipid vesicles in the presence of high salt. Hence, loss of antibacterial activity in the presence of salt would arise due to the inability of the peptides to associate with bacterial membranes which are rich in PE and PG.

We examined the ability of the peptides to permeabilize membranes by monitoring the dissipation of diffusion potential created by valinomycin (*46*) (Figure 10). It is evident that all of the peptides do permeabilize lipid vesicles. Membrane permeabilization was not observed with PC vesicles. Since antibacterial activity of the peptides was inhibited by high salt concentrations, the experiments were carried out in the absence of salt. The absence of a compensating concentration of salt in the external medium would lead to membrane tension induced by osmotic swelling of vesicles (*68*). Osmotically induced membrane tension in lipid vesicles modulates membrane permeabilization by lytic peptides (*68*). However, it is unlikely that osmotically induced membrane tension alone is the cause for membrane activity as the peptides do not permeabilize PC vesicles.

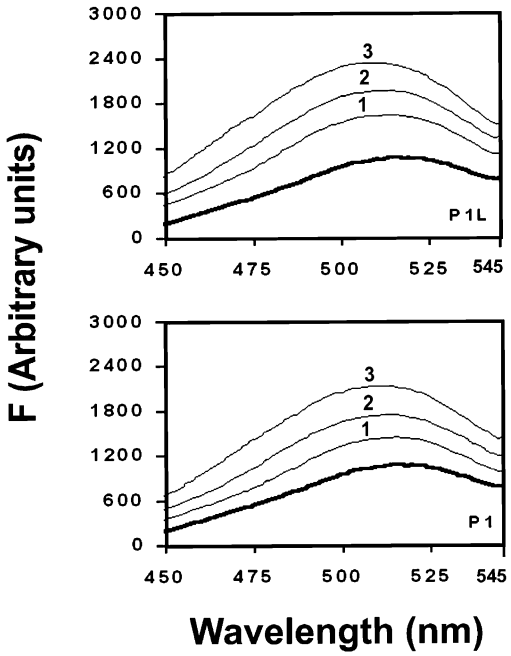

FIGURE 9: Interaction of peptides with PE:PG (3:1) LUV doped with dansyl-PE. Increasing concentrations of peptide were added to the lipid vesicles (lipid concentration = 50 μM). Spectra were obtained with the excitation wavelength at 280 nm. Key: (dark line) lipid blank; (thin lines with numbers above the traces) in the presence of peptides at peptide:lipid ratios of (1) 1:60, (2) 1:30, and (3) 1:15.

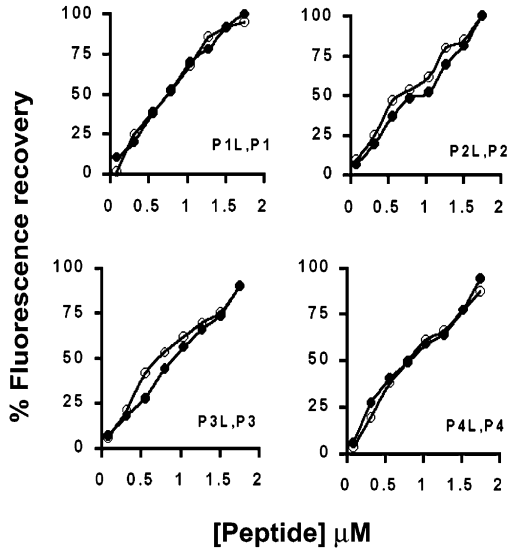

FIGURE 10: Maximal dissipation of diffusion potential in PE:PG vesicles induced by peptides. The peptides were added to LUV (lipid concentration = 25 μM) in K^+-free buffer preequilibrated with the fluorescent dye diS-C_3-(5) and valinomycin. Fluorescence recovery was measured 10 min after peptides were mixed with the vesicles. Key: (○) linear peptides; (●) cyclic peptides.

Binding of peptides P1−P4 as well as their linear forms to lipid vesicles composed of PE:PG (3:1) causes membrane destablization resulting in membrane permeabilization.

The β-hairpin structure at the C-terminus is conserved in α- and β-defensins. The β-hairpin structure is stabilized by the three disulfide bridges. In α- and β-defensins, all of the three disulfide bridges as well as the disulfide connectivities observed in the native sequence are not essential for manifestation of antibacterial activity (*30*−*32*). In a recent

report, it has been demonstrated that a synthetic peptide corresponding to an intragenic polymorphic form of human β-defensin-1 (hBD-1) where the disulfide connectivities are C_1-C_2 and C_3-C_5 (this form has five instead of six cysteines present in hBD-1) shows antibacterial activity (*56*). We have attempted to stabilize the β-hairpin conformation in the peptide segment corresponding to the C-terminal segment of BNBD-2 by introducing ^{D}PG and switching a GP sequence to PG. We have observed that this incorporation does stabilize the β-hairpin conformation. However, a rigid β-hairpin conformation and the presence of a disulfide bridge do not appear to be essential for antibacterial activity in synthetic peptides spanning the C-terminal segment of BNBD-2. The peptides interact with zwitterionic and negatively charged vesicles but with different orientations. However, permeabilization is observed only with PE:PG vesicles, consistent with the observations on α-defensins (*59*−*62*). Fluorescence data suggest that the peptides are oriented on the surface of the bilayer and cause membrane destabilization by electrostatic interactions rather than by a mechanism involving pore formation as proposed for magainin and other membrane-active antibacterial peptides (*69*, *70*). There is increasing evidence that defensins also participate in other aspects of innate immunity such as activation of mast cells and induction of cytokines (*4*−*6*). Defensins also appear to have a role in adaptive microbial immunity (*7*). Since the β-hairpin-forming segment of defensins exhibits antibacterial activity, it is conceivable that they may be able to induce the other physiological effects of defensins. Hence, short peptides corresponding to the C-terminal segments of defensins with appropriately positioned D-amino acids could have potential as therapeutic agents as they would be convenient to synthesize and also be more resistant to degradation by proteases.

ACKNOWLEDGMENT

We thank Dr. M. Vairamani, Indian Institute of Chemical Technology, for mass spectral analysis.

REFERENCES

1. Lehrer, R. I., Lichtenstein, A. K., and Ganz, T. (1993) *Annu. Rev. Immunol. 11*, 105−128.
2. Ouellette, A. J., and Selsted, M. E. (1996) *FASEB J. 10*, 1280−1289.
3. White, S. H., Wimley, W. C., and Selsted, M. E. (1995) *Curr. Opin. Struct. Biol. 5*, 521−527.
4. van Wetering, S., Sterk, P. J., Rabe, K. F., and Hiemstra, P. S. (1999) *J. Allergy Clin. Immunol.*, 1131−1138.
5. Lehrer, R. I., and Ganz, T. (1999) *Curr. Opin. Immunol. 11*, 23−27.
6. Lehrer, R. I., and Ganz, T. (2002) *Curr. Opin. Immunol. 14*, 96−102.
7. Yang, D., Biragyn, A., Kwak, L. W., and Oppenheim, J. J. (2002) *Trends Immunol. 23*, 291−296.
8. Tang, Y. Q., Yuan, J., Osapay, G., Osapay, K., Tran, D., Miller, C. J., Ouellette, A. J., and Selsted, M. E. (1999) *Science 286*, 498−502.
9. Leonova, L., Kokryakov, V. N., Aleshina, G., Hong, T., Nguyen, T., Zhao, C., Waring, A. J., and Lehrer, R. I. (2001) *J. Leukocyte Biol. 70*, 461−464.
10. Tran, D., Tran, P. A., Tang, Y.-Q., Yuan, J., Cole, T., and Selsted, M. E. (2002) *J. Biol. Chem. 277*, 3079−3084.
11. Pardi, A., Hare, D. R., Selsted, M. E., Morrison, R. D., Bassolino, D. A., and Bach, A. C., II (1988) *J. Mol. Biol. 201*, 625−636.
12. Zhang, X. L., Selsted, M. E., and Pardi, A. (1992) *Biochemistry 31*, 11348−11356.
13. Skalicky, J. J., Selsted, M. E., and Pardi, A. (1994) *Proteins: Struct., Funct., Genet. 20*, 52−67.
14. Zimmermann, G. R., Legault, P., Selsted, M. E., and Pardi, A. (1995) *Biochemistry 34*, 13663−13671.
15. Sawai, M. V., Jia, H. P., Liu, L., Aseyev, V., Wiencek, J. M., McCray, P. B., Jr., Ganz, T., Kearney, W. R., and Tack, B. F. (2001) *Biochemistry 40*, 3810−3816.
16. Hill, C. P., Yee, J., Selsted, M. E., and Eisenberg, D (1991) *Science 251*, 1481−1485.
17. Hoover, D. M., Rajashankar, K. R., Blumenthal, R., Puri, A., Oppenheim, J. J., Chertov, O., and Lubkowski, J. (2000) *J. Biol. Chem. 275*, 32911−32918.
18. Hoover, D. M., Chertov, O., and Lubkowski, J. (2001) *J. Biol. Chem. 276*, 39021−39026.
19. Selsted, M. E., Brown, D. M., DeLange, R. J., Harwig, S. S., and Lehrer, R. I. (1985) *J. Biol. Chem. 260*, 4579−4584.
20. Daher, K. A., Lehrer, R. I., Ganz, T., and Kroenberg, M. (1988) *Proc. Natl. Acad. Sci. U.S.A. 85*, 7327−7331.
21. Yamashita, T., and Saito, K. (1989) *Infect. Immun. 57*, 2405−2409.
22. Eisenhauer, P. B., Harwig, S. S., Szklarek, D., Ganz, T., Selsted, M. E., and Lehrer, R. I. (1989) *Infect. Immun. 57*, 2021−2027.
23. Selsted, M. E., Tang, Y. Q., Morris, W. L., McGuire, P. A., Novotny, M. J., Smith, W., Henschen, A. H., and Cullor, J. S. (1993) *J. Biol. Chem. 268*, 6641−6648.
24. Ouellette, A. J., Hsieh, M. M., Nosek, M. T., Gauci, D. F. C., Huttner, K. M., Buick, R. N., and Selsted, M. E. (1994) *Infect. Immun. 62*, 5040−5047.
25. Mak, P., Wojcik, K., Thogersen, I. B., and Dubin, A. (1996) *Infect. Immun. 64*, 4444−4449.
26. Shimoda, M., Ohki, K., Shimamoto, Y., and Kohashi, O. (1995) *Infect. Immun. 63*, 2886−2891.
27. Goldman, M. J., Anderson, G. M., Stolzenberg, E. D., Kari, U. P., Zasloff, M., and Wilson, J. M. (1997) *Cell 88*, 553−560.
28. Singh, P. K., Jia, H. P., Wiles, K., Hesselberth, J., Liu, L., Conway, B.-A., Greenberg, E. P., Valore, E. V., Welsh, M. J., Ganz, T., Tack, B. F., and McCray, P. B., Jr. (1998) *Proc. Natl. Acad. Sci. U.S.A. 95*, 14961−14966.
29. Bals, R., Wang, X., Wu, Z., Freeman, T., Bafna, V., Zasloff, M., and Wilson, J. M. (1998) *J. Clin. Invest. 102*, 874−880.
30. Thennarasu, S., and Nagaraj, R. (1999) *Biochem. Biophys. Res. Commun. 254*, 281−283.
31. Mandal, M., and Nagaraj, R. (2002) *J. Pept. Res. 59*, 95−104.
32. Mandal, M., Jagannadham, M. V., and Nagaraj, R. (2002) *Peptides 23*, 413−418.
33. Sibanda, B. L., Blundell, T. L., and Thornton, J. M. (1989) *J. Mol. Biol. 206*, 759−777.
34. Gunasekaran, K., Ramakrishnan, C., and Balaram, P. (1997) *Protein Eng. 10*, 1131−1141.
35. Blanco, F., Ramirez-Alvarado, M., and Serrano, L. (1998) *Curr. Opin. Struct. Biol. 8*, 107−111.
36. Haque, T. S., Little, J. C., and Gellman, S. H. (1994) *J. Am. Chem. Soc. 116*, 4105−4106.
37. Haque, T. S., Little, J. C., and Gellman, S. H. (1996) *J. Am. Chem. Soc. 118*, 6975−6985.
38. Haque, T. S., and Gellman, S. H. (1997) *J. Am. Chem. Soc. 119*, 2303−2304.
39. Karle, I. L., Awasthi, S. K., and Balaram, P. (1996) *Proc. Natl. Acad. Sci. U.S.A. 93*, 8189−8193.
40. Stanger, H. E., and Gellman, S. H. (1998) *J. Am. Chem. Soc. 120*, 4236−4237.
41. Das, C., Raghothama, S., and Balaram, P. (1998) *J. Am. Chem. Soc. 120*, 5812−5813.
42. Atherton, E., and Sheppard, R. C.(1989) *Solid-phase synthesis*: *a practical approach*, IRL Press, Oxford.
43. Veber, D. F., Milkowski, J. D., Varga, S. L., Denkewalter, R. G., and Hirschmann, R. (1972) *J. Am. Chem. Soc. 94*, 5456−5461.
44. Tam, J. P., Wu, C.-R., Liu, W., and Zhang, J.-W. (1991) *J. Am. Chem. Soc. 113*, 6657−6662.
45. MacDonald, R. C., MacDonald, R. I., Menco, B. P., Takeshita, K., Subbarao, N. K., and Hu, L.-R. (1991) *Biochim. Biophys. Acta 1061*, 297−303.
46. Sims, P. J., Waggoner, A. S., Wang, C. H., and Hoffman, J. F. (1974) *Biochemistry 13*, 3315−3329.
47. Hoyt, D. W., Cyr, D. M., Gierasch, L. M., and Douglas, M. G. (1991) *J. Biol. Chem. 266*, 21693-21699.
48. Watson, R. M., Woody, R. W., Lewis, R. V., Bohle, D. S., Andreotti, A. H., Ray, B., and Miller, K. W. (2001) *Biochemistry 40*, 14037−14046.

49. Krishna, A. G., Menon, S. T., Terry, T. J., and Sakmar, T. P. (2002) *Biochemistry 41*, 8298−8309.
50. Venkatraman, J., Gowda, G. A. N., and Balaram, P. (2002) *Biochemistry 41*, 6631−6639.
51. Blanco, F. J., Jimenez, M. A., Pineda, A., Rico, M., Santoro, J., and Nieto, J. L. (1994) *Biochemistry 33*, 6004−6014.
52. Blanco, F. J., and Serrano, L. (1995) *Eur. J. Biochem. 230*, 634−649.
53. Viguera, A. R., Jimenez, M. A., Rico, M., and Serrano, L. (1996) *J. Mol. Biol. 255*, 507−521.
54. Rao, A. G., Rood, T., Maddox, J., and Duvick, J. (1992) *Int. J. Pept. Protein Res. 40*, 507−514.
55. Dawson, N. F., Craik, D. J., McManus, A. M., Dashper, S. G., Reynolds, E. C., Tregear, G. W., Otvos, L., Jr., and Wade, J. D. (2000) *J. Pept. Sci. 6*, 19−25.
56. Circo, R., Skerlavaj, B., Gennaro, R., Amoroso, A., and Zanetti, M. (2002) *Biochem. Biophys. Res. Commun. 293*, 586−592.
57. Weiss, T. M., Yang, L., Ding, L., Waring, A. J., Lehrer, R. I., and Huang, H. W. (2002) *Biochemistry 41*, 10070−10076.
58. Kagan, B. L., Selsted, M. E., Ganz, T., and Lehrer, R. I. (1990) *Proc. Natl. Acad. Sci. U.S.A. 87*, 210−214.
59. Wimley, W. C., Selsted, M. E., and White S. H. (1994) *Protein Sci. 3*, 1362−1373.
60. Lohner, K., Latal, A., Lehrer, R. I., and Ganz, T. (1997) *Biochemistry 36*, 1525−1531.
61. Hristova, K., Selsted, M. E., and White, S. H. (1996) *Biochemistry 35*, 11888−11894.
62. Hristova, K., Selsted, M. E., and White, S. H. (1997) *J. Biol. Chem. 272*, 24224−24233.
63. Sillen, A., Diaz, J. F., and Engelborghs, Y. (2000) *Protein Sci. 9*, 158−169.
64. Adams, P. D., Chen, Y., Ma, K., Zagorski, M. G., Sonnichsen, F. D., McLaughlin, M. L., and Barkley, M. D. (2002) *J. Am. Chem. Soc. 124*, 9278−9286.
65. de Kroon, A. I. P. M., Soekarjo, M. W., de Gier, J., and de Kruijff, B. (1990) *Biochemistry 29*, 8229−8240.
66. Yeager, M. D., and Feigenson, G. W. (1990) *Biochemistry 29*, 4380−4392.
67. van Heusden, H. E., de Kruijff, B., and Breukink, E. (2002) *Biochemistry 41*, 12171−12178.
68. Polozov, I. V., Anantharamaiah, G. M., Segrest, J. P., and Epand, R. M. (2001) *Biophys. J. 81*, 949−959.
69. Matsuzaki, K. (1998) *Biochim. Biophys. Acta 1376*, 391−400.
70. McElhaney, R. N., and Prenner, E. J., Eds. (1999) *Biochim. Biophys. Acta* (reviews).

BI034403Y